PHYSICAL REVIEW C **85**, 032801(R) (2012)

Maximum mass and radius of neutron stars, and the nuclear symmetry energy

S. Gandolfi,[1] J. Carlson,[1] and Sanjay Reddy[1,2]
[1]*Theoretical Division, Los Alamos National Laboratory, Los Alamos, New Mexico 87545, USA*
[2]*Institute for Nuclear Theory, University of Washington, Seattle, Washington 98195-1550, USA*
(Received 2 March 2011; published 9 March 2012)

We calculate the equation of state of neutron matter with realistic two- and three-nucleon interactions using quantum Monte Carlo techniques and illustrate that the short-range three-neutron interaction determines the correlation between neutron matter energy at nuclear saturation density and higher densities relevant to neutron stars. Our model also makes an experimentally testable prediction for the correlation between the nuclear symmetry energy and its density dependence—determined solely by the strength of the short-range terms in the three-neutron force. The same force provides a significant constraint on the maximum mass and radius of neutron stars.

DOI: 10.1103/PhysRevC.85.032801 PACS number(s): 21.65.Cd, 21.65.Ef, 26.60.Kp

Since their discovery, neutron stars have remained our sole laboratory to study matter at supra-nuclear density and relatively low temperature. The equation of state (EoS) of matter at these densities is largely unknown but uniquely determines the structure of neutron stars and the relation between their mass (M) and radius (R). Matter that can support large pressure for a given energy density (typically called a stiff EoS) will favor large neutron star radii for a given mass. Such an EoS also predicts large values for the maximum mass of a neutron star that is stable with respect to gravitational collapse to a black hole. Conversely, a high-density phase that predicts a smaller pressure will result in more compact neutron stars and smaller maximum masses.

The recent accurate measurement of a large neutron star mass $M = 1.97 \pm 0.04 M_{\rm solar}$ in the system J1614-2230 provides strong evidence that the high-density equation of state is stiff [1]. Interestingly, attempts to infer neutron star radii have favored relatively small values ranging from 9 to 12 km [2–4]. Although the radius inference depends on specific model assumptions, these smaller radii imply a soft EoS in the vicinity of nuclear saturation density. Taken together, they indicate that the EoS of dense matter makes a transition from soft to stiff at supra-nuclear density. In this Rapid Communication we show that the three-neutron force (3n) is the key microscopic ingredient that determines the nature of this transition.

The importance of three-body forces in nuclear physics is well known, and quantum Monte Carlo (QMC) calculations of light nuclei have clarified its structure and strength. However, in these systems the dominant three-body force acts between two neutrons and a proton or between two protons and a neutron. While the force among three neutrons is important in light neutron-rich nuclei, the short distance behavior is not easily accessible [5]. Properties of large neutron-rich nuclei are potentially sensitive to this interaction, especially if the symmetry energy provides a reliable measure of the energy difference between pure neutron matter and symmetric nuclear matter at saturation density. There has been much recent progress in both theory and experiments to measure the symmetry energy and its density dependence, as reviewed in Refs. [6,7]. The symmetry energy is expected to be in the range 32 ± 2 MeV. We explore this experimentally suggested range for the nuclear symmetry energy and show that a more precise determination is needed to adequately constrain the 3n interaction.

In this work we solve the nonperturbative many-body nuclear Hamiltonian using the auxiliary field diffusion Monte Carlo (AFDMC) [8] method. Its accuracy in studying nuclear systems has been tested in light nuclei [9]. The extension to include three-body forces in pure neutron-rich systems is straightforward with no additional approximations within the AFDMC technique [10], and a comparison with the Green's function Monte Carlo (GFMC) has been extensively tested in neutron drops [11]. We present results for the EoS of neutron matter using phenomenological two-neutron (2n) potentials, which provide an accurate description of nucleon-nucleon scattering data up to high energies, and study the role of the poorly constrained 3n interaction.

In earlier work it has been established that the EoS in the density regime (1–3)ρ_0 plays an essential role in determining the neutron star radius [12]. In this density regime, the 3n interaction plays a critical role because of a large cancellation between the attractive and repulsive parts of the 2n interaction arising from the long- and short-distance behavior, respectively. Consequently, we find that the neutron star radius for a canonical mass of $1.4 M_{\rm solar}$ is especially sensitive to the 3n interaction. Although matter in the neutron star will contain a small admixture of protons, here we calculate the EoS of pure neutron matter for the following reasons. First, the structure of the interactions between neutrons is simpler than those between neutron and protons. Second, these simpler interactions are amenable to QMC methods to solve the many-body problem as it is devoid of the complexities of the isospin-dependent spin-orbit and three-nucleon potentials and clustering effects likely in systems with protons. Third, the fraction of protons required to ensure stability is small and is typically less than 10%. Finally, since generically neutron matter has higher pressure than matter containing any fraction of protons or strangeness in the form of hyperons or kaons, our results provide stringent upper bounds on the neutron maximum mass and radius.

To compute the EoS for neutron stars it is necessary to describe the nucleon-nucleon interactions at short distances or large relative momenta up to $p \simeq 2p_{Fn} \simeq 660$ MeV$(\rho/\rho_0)^{1/3}$, where p_{Fn} is the Fermi momentum, ρ is the typical density in the neutron star core, and $\rho_0 = 0.16$ fm^{-3} is the nuclear saturation density. Relative momenta up to p_{Fn} are required in even a mean-field (Fermi gas) description, and the nn interaction scatters nucleons to larger momenta up to order $(1.5\text{–}2)p_{Fn}$ at saturation density. Descriptions of higher density neutron matter with softer interactions if they are consistently evolved to lower scales, must include 3n (and potentially 4n) interactions.

Phenomenological two-nucleon potentials such as the Argonne potential have been constructed to describe scattering data up to relative momenta ≃600 MeV with high accuracy [13]. Despite the fact that the Argonne potential has been fit up to laboratory energies of 350 MeV, it very well reproduces scattering data up to much larger energies [14]. The AV8' interaction we employ in this study is identical to the full AV18 interaction in s and p waves and includes the dominant one-pion interaction in higher partial waves. Chiral interactions also reproduce the scattering data very well below 350 MeV laboratory energy, but they fail rapidly above because of the cutoff in presently available interactions. At larger momentum transfer, the potentials cannot describe inelasticities, but in scattering channels where inelasticities are known to be small they have been shown to provide a good description. They also provide good predictions [15] of high-momentum components of nuclear wave functions as observed in nucleon [16,17] and electron scattering [18,19]. These high-momentum observables provide a test of the assumed short-distance features. In the low-energy high-momentum region relevant to neutron stars the inelasticities in 2n scattering must be absorbed into many-body forces (3n, 4n,...) intimately connected to the short-distance behavior of the 2n interaction.

The nuclear Hamiltonians we consider contain the nonrelativistic kinetic energy and the 2n and 3n interactions:

$$H = -\frac{\nabla^2}{2m} + V_{2n} + V_{3n}. \tag{1}$$

For the 2n potential, we use the Argonne AV8$'$ model [20] and the form of the 3n interaction is inspired by both the Urbana IX and the Illinois models [5]. We consider a range of 3n interactions that contain long-distance s- and p-wave 2π exchange contributions, an intermediate-range (3π loops) contribution, and a spin-independent short-range repulsive term. Explicitly,

$$V_{3N} = A_{2\pi}^{PW}\mathcal{O}^{2\pi,PW} + A_{2\pi}^{SW}\mathcal{O}^{2\pi,SW} + A_{3\pi}\mathcal{O}^{3\pi} + A_R\mathcal{O}^R. \tag{2}$$

This form of interaction includes all the terms present in low-order chiral interaction, plus selected terms found to be important in studies of light nuclei and nuclear matter using the Argonne interactions.

The structure of the operators $\mathcal{O}$ appearing above are defined in Ref. [5]. The relative contributions of these four components of the 3n force depends on the 2n interaction. We find that, for the Argonne potential, the 2n interactions suppress the long-distance (2π) contribution of the 3n force in the ground state. This suppression is a result of the pion-range correlations induced by the 2n force; we find it also occurs for the super-soft core NN interaction [21]. For typical ranges of values of the strength parameters $A_{2\pi}^{PW}$ and $A_{2\pi}^{SW}$ considered in Ref. [5] we find the contribution of these operators to the ground-state energy is repulsive but very small at all densities studied. In contrast, this interaction is large and attractive in light nuclei where both neutrons and protons contribute. The intermediate-range (3π) 3n interaction was introduced to fit the properties of weakly bound neutron-rich nuclei such as ^{8}He [5]. Earlier calculations [10] have shown that this interaction is strong and attractive in neutron matter for typical values of $A_{3\pi}$ quoted in Ref. [5]. In this work, we explored a range of values for $A_{3\pi}$ from zero to that in the Illinois-7 3n interaction [22] because the structure of this term is still not fully understood or constrained. We use a phenomenological short-range repulsive term as in the Urbana and Illinois three-body forces, with $V_R = A_R\mathcal{O}^R = A_R\sum_{cyc}T^2(m_\pi r_{ij})T^2(m_\pi r_{jk})$, where the function $T(x)$ is defined in Ref. [5]. We have also considered a different form $V_\mu^R = A_R\sum_{cyc}v(r_{ij})v(r_{jk})$ with and $v(r) = \exp(-2\mu r)$; other different forms of V_R have been explored, giving very similar results.

The 3n interaction we employ is not intended to be a microscopic treatment of the complete 3n interaction. It assumes that for the neutron matter equation of state the effects of more complicated spin-dependent short-distance 3n interactions, relativistic effects, and potential 4n interactions can be mimicked with simplified three-neutron interactions with a wide range of spatial dependence. This assumption has been tested in the case of relativistic corrections, where in Ref. [23] it was found that the density dependence of the relativistic effects is similar to that of the 3n interaction. Further tests of the density dependence of specific higher-order terms in the chiral interaction are valuable. The different forms of V_R we have explored span a wide range of density dependence for the 3n interaction, as shown below.

For the 3n interaction we vary both $A_{3\pi}$ and μ to study the sensitivity to short-range physics. The strength of the short-range 3n interaction A_R is taken to be a free parameter adjusted to yield the experimentally accessible nuclear symmetry energy. Although not proven, we make the following reasonable assumptions: (1) relativistic effects in neutron matter show a similar density dependence to the short-range three-nucleon interaction as carefully studied in Ref. [23], (2) the density dependence of additional spin-dependent short-range 3n interactions (for example, higher-order terms in chiral expansions) in the equation of state of neutron matter can be described in a spin-independent model, and (3) four-nucleon force contributions with different density dependence are suppressed relative to the 3n force for densities up to $(2\text{–}3)\rho_0$. This last assumption can be justified at nuclear density by the high-precision fits to light-nuclei obtained with only 3n forces [24]; at higher density this model assumption can be tested by its predicted correlation between properties of neutron-rich nuclei and neutron stars.

We assume that $E_{\rm sym} = E_{\rm neutron}(\rho_0) - E_{\rm nuclear}(\rho_0)$ and using experimental values of $E_{\rm sym} = 32 \pm 2$ MeV [25] and $E_{\rm nuclear}(\rho_0) = -16.0 \pm 0.1$ MeV from nuclear masses models

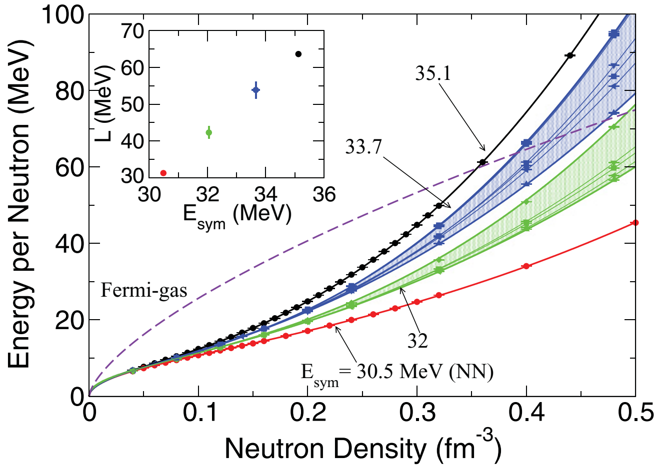

FIG. 1. (Color online) The energy per particle of neutron matter for different values of the nuclear symmetry energy (E_{sym}). For each value of E_{sym} the corresponding band shows the effect of different spatial and spin structures of the three-neutron interaction. The inset shows the linear correlation between E_{sym} and its density derivative L.

[26] we obtain an empirical constraint for neutron matter energy $E_{\mathrm{neutron}}(\rho_0) = 16 \pm 2$ MeV. Potential higher-order corrections to the quadratic nuclear symmetry energy, for which there is some theoretical motivation but no clear experimental evidence, may affect the extraction of the neutron matter energy and increase the associated error. In this work we ignore these poorly known corrections and tune A_R to reproduce the neutron matter energy in the range 16 ± 2 MeV. Our results are shown in Fig. 1, where the green and blue points are QMC results for different choices of A_R corresponding to $E_{\mathrm{neutron}}(\rho_0) = 16$ MeV($E_{\mathrm{sym}} = 32$ MeV) and $E_{\mathrm{neutron}}(\rho_0) = 17.7$ MeV($E_{\mathrm{sym}} = 33.7$ MeV), respectively. The results are compared to those obtained using a 2n force without 3n ($E_{\mathrm{sym}} = 30.5$ MeV) and 2n combined with the Urbana IX 3n ($E_{\mathrm{sym}} = 35.1$ MeV). The bands depict the sensitivity to short-distance spin and spatial structure of the 3n interaction and are obtained by varying the range of the 3n short-distance force and $A_{3\pi}$.

In the vicinity of nuclear density, $E_{\mathrm{neutron}}(\rho) = E_{\mathrm{neutron}}(\rho_0) + L/3(\rho - \rho_0)/\rho_0$, where L is related to the derivative of the nuclear symmetry energy. The inset in Fig. 1 shows the correlation between E_{sym} and L. This correlation is insensitive to the large variations in the range of the short-range 3n force μ and the strength of the 3π term $A_{3\pi}$. This is in sharp contrast to the predictions of mean-field theories where the slope was found to be very sensitive to the choice of effective interactions [27]. Previous calculations of neutron matter up to ρ_0 [28] use a chiral 2n interaction fit to laboratory energies of 350 MeV plus the two-pion exchange three-nucleon interaction to calculate the neutron matter equation of state using perturbation theory. In contrast to our results, a significant repulsion from the 2π exchange long-range 3n interaction was found. Since this force is better constrained by light nuclei, these earlier calculations can make a prediction for the neutron matter energy independent of the phenomenological short-range interaction, which plays an important role in our calculation. To understand this basic difference, further tests of the convergence of perturbation theory and the chiral expansion in the diagrammatic calculations, a survey of other two-body interactions in the AFDMC, and the incorporation of chiral interactions in nonperturbative methods such as lattice and suitable extension of QMC would be necessary.

TABLE I. Fitting parameters for the neutron matter EoS defined in Eq. (3) for selected different Hamiltonians.

3N force	E_{sym} (MeV)	L (MeV)	a (MeV)	α	b (MeV)	β
none	30.5	31.3	12.7	0.49	1.78	2.26
$V_{2\pi}^{PW} + V_{\mu=150}^{R}$	32.1	40.8	12.7	0.48	3.45	2.12
$V_{2\pi}^{PW} + V_{\mu=300}^{R}$	32.0	40.6	12.8	0.488	3.19	2.20
$V_{3\pi} + V_R$	32.0	44.0	13.0	0.49	3.21	2.47
$V_{2\pi}^{PW} + V_{\mu=150}^{R}$	33.7	51.5	12.6	0.475	5.16	2.12
$V_{3\pi} + V_R$	33.8	56.2	13.0	0.50	4.71	2.49
UIX	35.1	63.6	13.4	0.514	5.62	2.436

Current determinations of L have relied on analysis of neutron skins, surface contributions to the symmetry energy of neutron-rich nuclei, and isospin diffusion in heavy-ion reactions. These studies have been useful but not very constraining as acceptable values are in the range $L = 40$–100 MeV [25]. However, a better determination of L even with modest reduction in the error would test our model for 2n and 3n interactions.

The predictions of QMC can be accurately fit using

$$E(\rho) = a\left(\frac{\rho}{\rho_0}\right)^{\alpha} + b\left(\frac{\rho}{\rho_0}\right)^{\beta}, \tag{3}$$

where the coefficients a and α are sensitive to the low-density behavior of the EoS, while b and β are sensitive to the high-density physics [29]. We find that the 3n force plays a key role in determining the coefficient b and the variation of the other EoS parameters is comparatively small. Numerical values for these parameters are reported in Table I for selected Hamiltonians.

To calculate the mass and radius of neutron stars we solve the Tolman-Oppenheimer-Volkoff (TOV) equations for the hydrostatic structure of a spherical nonrotating star using the QMC equation of state for neutron matter [30,31]. The QMC EoS we use is for $\rho \geqslant \rho_{\mathrm{crust}} = 0.08$ fm^{-3}. Below this density we use the EoS of the crust obtained in earlier works in Refs. [32,33].

The neutron star mass-radius predictions are obtained by varying the 3n force and are shown in Fig. 2. The striking feature is the estimated error in the neutron star radius with a canonical mass of $1.4M_{\mathrm{solar}}$. The uncertainty in the measured symmetry energy of ± 2 MeV leads to an uncertainty of about 3 km for the radius, while the uncertainties in the short-distance structure of the 3n force predicts a radius uncertainty of $\lesssim 1$ km. The different bands of Fig. 2 correspond to the EoS of Fig. 1 with the same colors, giving different values of E_{sym}.

The central density of stars with $M \gtrsim 1.5M_{\mathrm{solar}}$ are larger than $3\rho_0$. At these higher densities, effects such as relativistic corrections to the kinetic energy, retardation in the potential,

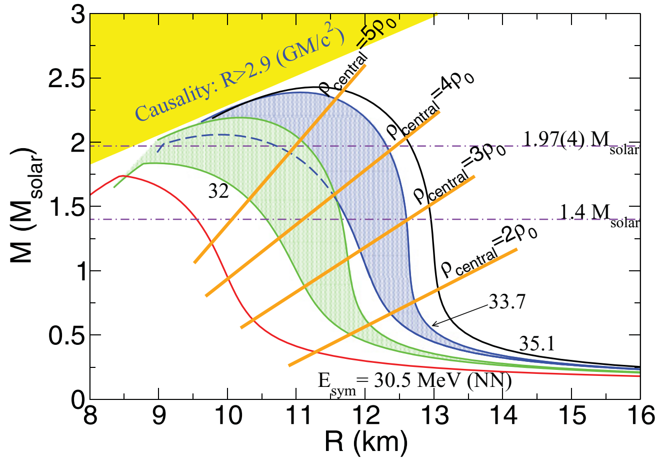

FIG. 2. (Color online) Mass-radius relation for the EoS with three-neutron interactions corresponding to the bands for different $E_{\rm sym}$ shown in Fig. 1. The intersections with the orange lines roughly indicate central densities realized in these stars.

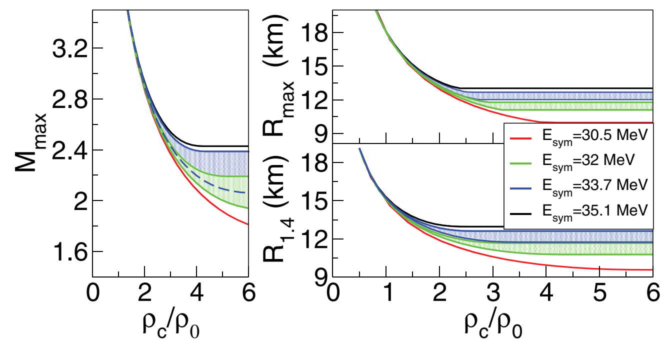

FIG. 3. (Color online) Bounds on the maximum mass and radius for different equations of state as a function of the critical density ρ_c. The left panel shows the maximum mass; the right top and bottom panels show the maximum possible radius for any neutron star with mass greater than $1.2M_{\rm solar}$ and for a neutron star with $M = 1.4M_{\rm solar}$, respectively.

and four- and higher body forces become important. Consequently, nonrelativistic models violate causality and predict a sound speed $c_s = \sqrt{\partial p/\partial \epsilon} \gtrsim c$ for $\rho \simeq (4\text{–}5)\rho_0$. To overcome this deficiency we adopt the strategy suggested in Ref. [34] and replace the EoS above a critical density ρ_c by the maximally stiff or causal EoS given by $p(\epsilon) = c^2\epsilon - \epsilon_c$, where p is the pressure, ϵ is the energy density, c is the speed of light, and ϵ_c is a constant. This EoS is maximally stiff and predicts the most rapid increase of pressure with energy density without violating causality. The constant ϵ_c is the parameter that determines the discontinuity in energy density between the low- and high-density equations of state. Our choice of ϵ_c ensures that the energy density is continuous and provides an upper bound on both the radius and the maximum mass of the neutron star.

Figure 3 shows how the bounds on the maximum radius and mass of the neutron star vary with our choice of the critical density ρ_c. It also illustrates that the bounds provide useful constraints only when the EoS is known up to $(2\text{–}3)\rho_0$. In Ref. [35] bounds on the radius were derived by using an EoS of neutron matter calculated up to ρ_0 with specific assumptions about polytropic equations of state at higher densities. Our upper bounds are model independent and show that the radius of a $1.4M_{\rm solar}$ neutron star can be as large as 16 km if $\rho_c = \rho_0$. To obtain a tighter bound the equation of state between $1\rho_0$ and $2\rho_0$ is important. The red, green, blue, and black curves are predictions corresponding to the 3n interaction strength fit to $E_{\rm sym} = 30.5, 32.0, 33.7$, and 35.1 MeV, respectively. We also note that these bounds do not change much for $\rho_c \gtrsim 4\rho_0$ because the QMC EoS is already close to being maximally stiff in this region. These upper bounds provide a direct relation between the experimentally measurable nuclear symmetry energy and the maximum possible mass and radius of neutron stars.

To summarize, we predict that the correlation between the symmetry energy and its derivative at nuclear density is nearly independent of the detailed short-range 3n force once its strength is tuned to give a particular value of $E_{\rm sym}$. Consequently, in our model one short-distance parameter A_R completely determines the behavior of the EoS. At higher density, the sensitivity to short-distance behavior of the 3n interaction translates to an uncertainty of about 1 km for the neutron star radius with mass $M = 1.4M_{\rm solar}$. The uncertainty at high density due to a poorly constrained symmetry energy is larger, $\simeq$3 km. Within our model we predict that neutron star radii are in the 10–13 km range for nuclear symmetry energy in the range 32–34 MeV. If nuclear experiments can determine that $E_{\rm sym} \leqslant 32$ MeV, QMC predicts that $L \lesssim 45$ MeV at nuclear density, and for neutron stars it predicts $M_{\rm max} < 2.2M_{\rm solar}$ and $R < 12$ km for a neutron star with $M = 1.4M_{\rm solar}$. The relationship between the symmetry energy and its density dependence is experimentally relevant, and its implications on the neutron star mass-radius relationship are subject to clear observational tests.

We thank Bob Wiringa, Steve Pieper, Kevin Schmidt, and Francesco Pederiva for useful discussions. We also thank Chuck Horowitz, Jim Lattimer, Madappa Prakash, and Achim Schwenk for comments on an early version of the manuscript. This work was supported by a grant from the Department of Energy (DOE) under Contracts No. DE-FC02-07ER41457 (UNEDF SciDAC) and No. DE-AC52-06NA25396 (LANL) and the DOE topical collaboration to study “Neutrinos and nucleosynthesis in hot and dense matter.” Computer time was made available by Los Alamos Open Supercomputing and by the National Energy Research Scientific Computing Center (NERSC).

[1] P. B. Demorest, T. Pennucci, S. M. Ransom, M. S. E. Roberts, and J. W. T. Hessels, Nature (London) **467**, 1081 (2010).

[2] N. A. Webb and D. Barret, Astrophys. J. **671**, 727 (2007).

[3] T. Güver, P. Wroblewski, L. Camarota, and F. Özel, Astrophys. J. **719**, 1807 (2010).

[4] A. W. Steiner, J. M. Lattimer, and E. F. Brown, Astrophys. J. **722**, 33 (2010).

[5] S. C. Pieper, V. R. Pandharipande, R. B. Wiringa, and J. Carlson, Phys. Rev. C **64**, 014001 (2001).
[6] A. W. Steiner, M. Prakash, J. M. Lattimer, and P. J. Ellis, Phys. Rep. **411**, 325 (2005).
[7] D. V. Shetty, S. J. Yennello, and G. A. Souliotis, Phys. Rev. C **76**, 024606 (2007).
[8] K. E. Schmidt and S. Fantoni, Phys. Lett. B **446**, 99 (1999).
[9] S. Gandolfi, F. Pederiva, S. Fantoni, and K. E. Schmidt, Phys. Rev. Lett. **99**, 022507 (2007).
[10] A. Sarsa, S. Fantoni, K. E. Schmidt, and F. Pederiva, Phys. Rev. C **68**, 024308 (2003).
[11] S. Gandolfi, J. Carlson, and S. C. Pieper, Phys. Rev. Lett. **106**, 012501 (2011).
[12] J. M. Lattimer and M. Prakash, Astrophys. J. **550**, 426 (2001).
[13] R. B. Wiringa, V. G. J. Stoks, and R. Schiavilla, Phys. Rev. C **51**, 38 (1995).
[14] R. B. Wiringa (private communicaion) [http://www.phy.anl.gov/theory/research/av18/].
[15] R. Schiavilla, R. B. Wiringa, S. C. Pieper, and J. Carlson, Phys. Rev. Lett. **98**, 132501 (2007).
[16] E. Piasetzky, M. Sargsian, L. Frankfurt, M. Strikman, and J. W. Watson, Phys. Rev. Lett. **97**, 162504 (2006).
[17] A. Tang, J. W. Watson, J. Aclander, J. Alster, G. Asryan, Y. Averichev, D. Barton, V. Baturin, N. Bukhtoyarova, A. Carroll, S. Gushue, S. Heppelmann, A. Leksanov, Y. Makdisi, A. Malki, E. Minina, I. Navon, H. Nicholson, A. Ogawa, Y. Panebratsev, E. Piasetzky, A. Schetkovsky, S. Shimanskiy, and D. Zhalov, Phys. Rev. Lett. **90**, 042301 (2003).
[18] R. Subedi *et al.*, Science **320**, 1476 (2008).
[19] R. Shneor *et al.*, Phys. Rev. Lett. **99**, 072501 (2007).
[20] R. B. Wiringa and S. C. Pieper, Phys. Rev. Lett. **89**, 182501 (2002).
[21] S. C. Pieper and R. B. Wiringa (private communication).
[22] S. C. Pieper, AIP Conf. Proc. **1011**, 143 (2008).
[23] A. Akmal, V. R. Pandharipande, and D. G. Ravenhall, Phys. Rev. C **58**, 1804 (1998).
[24] E. Epelbaum, H.-W. Hammer, and Ulf-G. Meißner, Rev. Mod. Phys. **81**, 1773 (2009).
[25] M. B. Tsang, Y. Zhang, P. Danielewicz, M. Famiano, Z. Li, W. G. Lynch, and A. W. Steiner, Phys. Rev. Lett. **102**, 122701 (2009).
[26] P. Möller, J. R. Nix, W. D. Myers, and W. J. Swiatecki, At. Data Nucl. Data Tables **59**, 185 (1995).
[27] B. A. Brown, Phys. Rev. Lett. **85**, 5296 (2000).
[28] K. Hebeler and A. Schwenk, Phys. Rev. C **82**, 014314 (2010).
[29] S. Gandolfi, A. Yu. Illarionov, K. E. Schmidt, F. Pederiva, and S. Fantoni, Phys. Rev. C **79**, 054005 (2009).
[30] J. M. Lattimer and M. Prakash, Science **304**, 536 (2004).
[31] S. Gandolfi, A. Yu. Illarionov, S. Fantoni, J. C. Miller, F. Pederiva, and K. E. Schmidt, Mon. Not. R. Astron. Soc. **404**, L35 (2010).
[32] G. Baym, C. Pethick, and P. Sutherland, Astrophys. J. **170**, 299 (1971).
[33] J. W. Negele and D. Vautherin, Nucl. Phys. A **207**, 298 (1973).
[34] C. E. Rhoades and R. Ruffini, Phys. Rev. Lett. **32**, 324 (1974).
[35] K. Hebeler, J. M. Lattimer, C. J. Pethick, and A. Schwenk, Phys. Rev. Lett. **105**, 161102 (2010).